

## Supplemental Information

### Impact of Morphology on Polaron Delocalization in a Semicrystalline Conjugated Polymer

**Robert Steyrlleuthner<sup>1</sup>, Yuexing Zhang<sup>2,3</sup>, Lei Zhang<sup>4</sup>, Felix Kraffert<sup>1</sup>, Ben Cherniawski<sup>4</sup>, Robert Bittl<sup>1</sup>,  
Alejandro L. Briseno<sup>4</sup>, Jean-Luc Bredas<sup>2</sup>, Jan Behrends<sup>1</sup>**

[1] Freie Universität Berlin, Berlin Joint EPR Lab, Institut für Experimentalphysik, Berlin, Germany

[2] King Abdullah University of Science & Technology, Solar & Photovoltaics Engineering Research  
Center, Thuwal 23955-6900, Saudi Arabia

[3] Department of Chemistry, Hubei University, Wuhan 430062, China

[4] Department of Polymer Science and Engineering, Conte Research Center, University of  
Massachusetts, 120 Governors Drive, Amherst, MA, 01003, USA

#### Sample Preparation

The two molecular weight fractions of PBTTT were purchased from 1.Materials ( $M_n = 20$  kDa, PDI 2.4) and Sigma Aldrich ( $M_n = 15$  kDa, PDI 2.9) while [60]PCBM was obtained from Solenne BV. Undeuterated BTTT oligomers were synthesized as described previously.<sup>1</sup>

For the fabrication of the EPR samples the materials were dissolved in chloroform at a concentration of 20 g/l and 1:1 mixing ratio with [PCBM]. About 50  $\mu$ L of the solution were loaded under inert atmosphere into EPR quartz tubes with an outer diameter of 2.9 mm. The solvent was subsequently evaporated under vacuum, leaving a film on the inner sample tube wall. Subsequently, the tubes were filled with Helium up to a pressure of 500 mbar and sealed using a blowtorch.

The second type of samples, referred to as thin film samples, were prepared as described in the main text.

#### Electron Spin Resonance

Pulsed ENDOR experiments and field-swept echos have been performed at a microwave frequency of 34 GHz (Q-band) and a temperature of 10 K on a Bruker Elexsys E580 spectrometer and a home-built Q-band ENDOR resonator. Part of the ENDOR spectra were recorded with the Davies ENDOR pulse sequence  $\pi$ -T- $\pi/2$ - $\tau$ - $\pi$ - $\tau$ -echo with delay times T=24 ms  $\tau$ =350 ns. The length of the  $\pi$  inversion pulse was 128 ns. The RF-pulse during the delay time T was applied for 21 ms. All ENDOR spectra were recorded in stochastic mode, where the RF is varied randomly. The shot repetition time was chosen to maximize the inverted echo intensity (around 100000-200000  $\mu$ s). MIMS ENDOR spectra were recorded equally with spitting of the first  $\pi$  pulse into two  $\pi/2$  pulses separated by a delay time  $\tau$  and keeping the remaining parameters. For MIMS ENDOR  $\tau$  was chosen as described in the main text to avoid appearance of periodic blind spots in the spectra. Polarons were generated by constant illumination with a Schott KL2500 white light source through windows of cryostat and resonator.

#### Computational Methodology

All the neutral molecules and cations are assumed to have  $C_i$  symmetry (which we have checked does not impact the results to any significant extent but reduces greatly the computational costs). We

consider three optimally tuned range-separation (TRS) DFT methods, LC- $\omega$ PBE,<sup>2-5</sup> LC-BLYP,<sup>6</sup> and  $\omega$ B97XD<sup>7</sup>. 6-31G(d) basis set was used for all calculations. It is important to bear in mind that the default  $\omega$  values of range-separated DFT functions are generally too large when considering extended p-conjugated systems, which thus require  $\omega$  tuning.<sup>8-12</sup> The optimal  $\omega$  values are obtained by minimizing  $J(\omega)^2 = [\epsilon_H(N) + IP(N)]^2$  (where  $\epsilon_H$  is the (negative) energy of the highest occupied molecular orbital (HOMO) and IP is the vertical ionization potential) for a given N-electron system.<sup>9</sup> The minimization proceeds in the following way: A first  $\omega$  value is obtained based on the initial geometry; the geometry is then re-optimized with this  $\omega$  value and a new  $\omega$  value is optimized from the new geometry; this process is repeated until the  $\omega$  value converges (within a threshold of 0.0001 Bohr<sup>-1</sup>), which usually occurs after 3-4 iteration steps. In order to keep the same functional for a given oligomer, optimizations of the cations are performed with the tuned  $\omega$  value of the neutral molecule (and the 6-31G(d) basis set). All calculations were carried out with the Gaussian 09 package.<sup>13</sup>

### Supporting Data

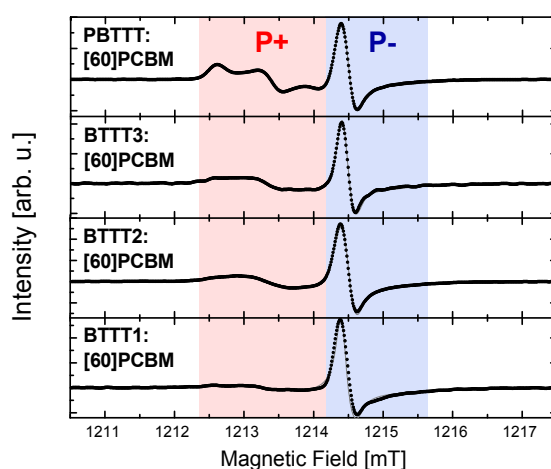


**Figure S1** Magnetic field-swept echo-detected spectra of the photogenerated polarons in BTTT oligomers and PBTTT mixed with [60]PCBM measured at 10 K.

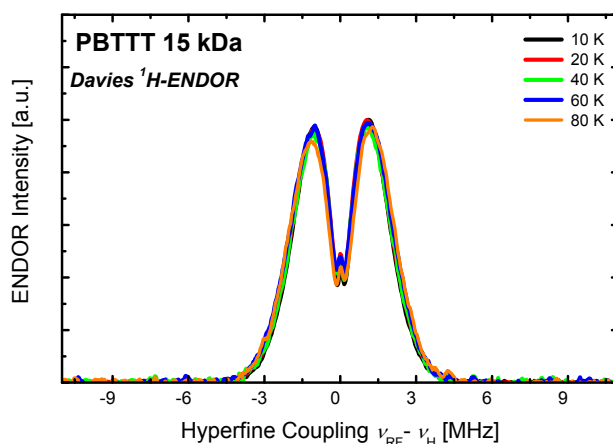


**Figure S2 a)** <sup>1</sup>H-Davies ENDOR spectra of PBTTT (15 kDa) in mixture with [60]PCBM measured at the magnetic field position of the positive polaron (128 ns inversion pulse) showing no change of the signature with increasing temperature.

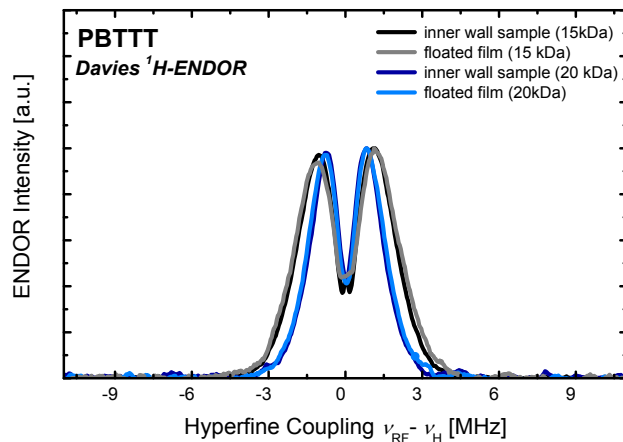


**Figure S3 a)**  $^1\text{H}$ -Davies ENDOR spectra of PBTTT (15 kDa and 20 kDa) in mixture with [60]PCBM measured at the magnetic field position of the positive polaron (128 ns inversion pulse, 10 K). The spectra show in general no significant difference between floated thin-film samples and thicker inner-wall samples, while the main effect can be attributed to the change in molecular weight of the PBTTT.

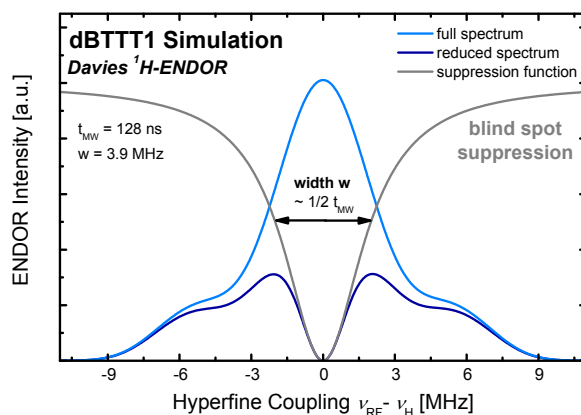


**Figure S4** Simulated  $^1\text{H}$ -Davies ENDOR spectra of dBTTT1 (128 ns inversion pulse) showing the influence of the blind spot on the ENDOR spectrum.

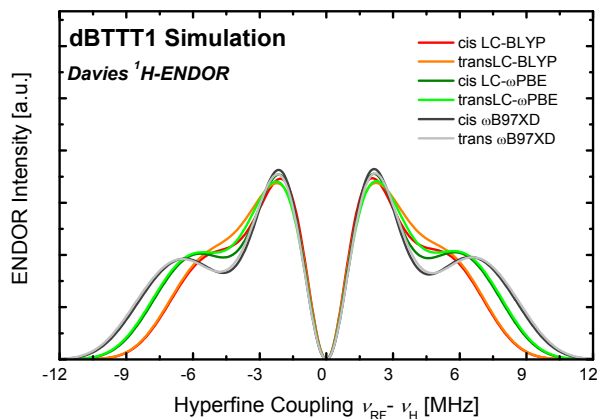


**Figure S5** Simulated  $^1\text{H}$ -Davies ENDOR spectra of dBTTT1 in (128 ns inversion pulse) in cis and trans conformation of the oligomer.

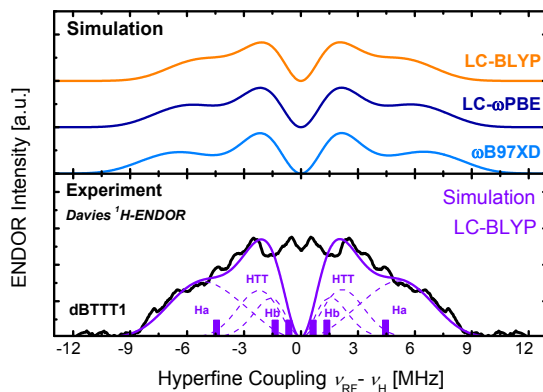


**Figure S6** The upper graph shows separate simulations of the BTTT1 cation  $^1\text{H}$  Davies ENDOR spectra considering three aromatic protons Ha, Hb, HTTT. The lower graph shows the complete simulation (violet) of the experimental BTTT1 spectrum (black) with LC-BLYP and the separate proton contributions. Violet bars represent the individual  $^1\text{H}$  isotropic couplings to simulate the spectrum. All simulated spectra include complete ENDOR effect suppression around  $a=0$  (Davies inversion  $\pi$ -pulse 128 ns).

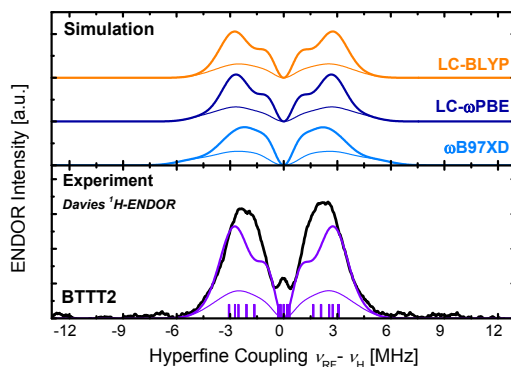


**Figure S7** The upper graph shows separate simulations of the BTTT2 cation  $^1\text{H}$  Davies ENDOR spectra considering five aromatic protons Ha, Hb, HTTT1, HTTT2, Hb' and the complete simulation including the HFC caused by side chain protons in coplanar arrangement. The lower graph shows the complete simulation (violet) of the experimental BTTT2 spectrum (black) with LC-BLYP. Violet bars represent the individual  $^1\text{H}$  isotropic couplings to simulate the spectrum. All simulated spectra include complete ENDOR effect suppression around  $a=0$  (Davies inversion  $\pi$ -pulse 128 ns).

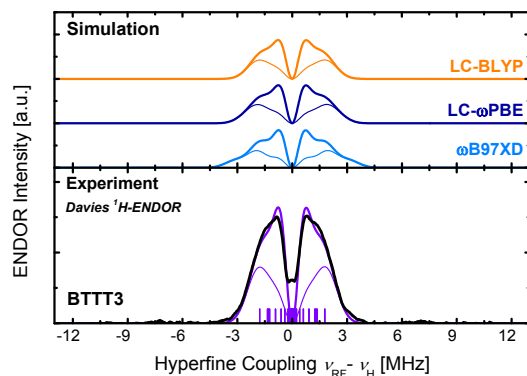


**Figure S8** The upper graph shows separate simulations of BTTT3 cation  $^1\text{H}$  Davies ENDOR spectra considering seven aromatic protons  $\text{H}_a$ ,  $\text{H}_b$ ,  $\text{H}_b'$ ,  $\text{H}_b''$ ,  $\text{HTTT1}$ ,  $\text{HTTT2}$ ,  $\text{HTTT3}$  (thin lines) and the complete simulation including the HFC caused by side chain protons in nearly perpendicular arrangement. The lower graph shows the complete simulation (violet) of the experimental BTTT3 spectrum (black) with LC-BLYP. Violet bars represent the individual  $^1\text{H}$  isotropic couplings to simulate the spectrum. All simulated spectra include complete ENDOR effect suppression around  $a=0$  (Davies inversion  $\pi$ -pulse 128 ns).

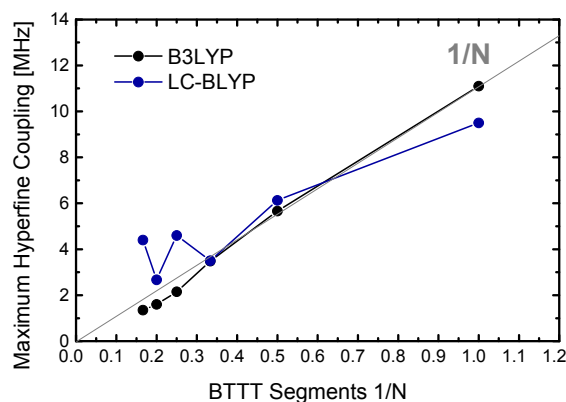


**Figure S9** Maximum  $^1\text{H}$  hyperfine coupling of BTTT oligomers calculated with B3LYP and LC-BLYP.

- (1) Zhang, L.; Liu, F.; Diao, Y.; Marsh, H. S.; Colella, N. S.; Jayaraman, A.; Russell, T. P.; Mannsfeld, S. C. B.; Briseno, A. L. *Journal of the American Chemical Society* **2014**, *136*, 18120.
- (2) Vydrov, O. A.; Scuseria, G. E.; Perdew, J. P. *The Journal of Chemical Physics* **2007**, *126*, 154109.
- (3) Vydrov, O. A.; Scuseria, G. E. *The Journal of Chemical Physics* **2006**, *125*, 234109.
- (4) Vydrov, O. A.; Heyd, J.; Krukau, A. V.; Scuseria, G. E. *The Journal of Chemical Physics* **2006**, *125*, 074106.
- (5) Tawada, Y.; Tsuneda, T.; Yanagisawa, S.; Yanai, T.; Hirao, K. *The Journal of Chemical Physics* **2004**, *120*, 8425.

- (6) Iikura, H.; Tsuneda, T.; Yanai, T.; Hirao, K. *The Journal of Chemical Physics* **2001**, *115*, 3540.
- (7) Chai, J.-D.; Head-Gordon, M. *Physical Chemistry Chemical Physics* **2008**, *10*, 6615.
- (8) Körzdörfer, T.; Brédas, J.-L. *Accounts of Chemical Research* **2014**, *47*, 3284.
- (9) Baer, R.; Livshits, E.; Salzner, U. *Annual Review of Physical Chemistry* **2010**, *61*, 85.
- (10) Wong, B. M.; Hsieh, T. H. *Journal of Chemical Theory and Computation* **2010**, *6*, 3704.
- (11) Körzdörfer, T.; Parrish, R. M.; Marom, N.; Sears, J. S.; Sherrill, C. D.; Brédas, J.-L. *Physical Review B* **2012**, *86*, 205110.
- (12) Sun, H.; Zhong, C.; Brédas, J.-L. *Journal of Chemical Theory and Computation* **2015**, *11*, 3851.
- (13) Frisch, M. J.; Trucks, G. W.; Schlegel, H. B.; Scuseria, G. E.; Robb, M. A.; Cheeseman, J. R.; Scalmani, G.; Barone, V.; Mennucci, B.; Petersson, G. A.; Nakatsuji, H.; Caricato, M.; Li, X.; Hratchian, H. P.; Izmaylov, A. F.; Bloino, J.; Zheng, G.; Sonnenberg, J. L.; Hada, M.; Ehara, M.; Toyota, K.; Fukuda, R.; Hasegawa, J.; Ishida, M.; Nakajima, T.; Honda, Y.; Kitao, O.; Nakai, H.; Vreven, T.; Montgomery Jr., J. A.; Peralta, J. E.; Ogliaro, F.; Bearpark, M. J.; Heyd, J.; Brothers, E. N.; Kudin, K. N.; Staroverov, V. N.; Kobayashi, R.; Normand, J.; Raghavachari, K.; Rendell, A. P.; Burant, J. C.; Iyengar, S. S.; Tomasi, J.; Cossi, M.; Rega, N.; Millam, N. J.; Klene, M.; Knox, J. E.; Cross, J. B.; Bakken, V.; Adamo, C.; Jaramillo, J.; Gomperts, R.; Stratmann, R. E.; Yazyev, O.; Austin, A. J.; Cammi, R.; Pomelli, C.; Ochterski, J. W.; Martin, R. L.; Morokuma, K.; Zakrzewski, V. G.; Voth, G. A.; Salvador, P.; Dannenberg, J. J.; Dapprich, S.; Daniels, A. D.; Farkas, Ö.; Foresman, J. B.; Ortiz, J. V.; Cioslowski, J.; Fox, D. J.; Gaussian, Inc.: Wallingford, CT, USA, 2009.